OPTIMIZATION OF ELECTRIC VEHICLE CHARGING MANAGEMENT WITH DISTRIBUTIONAL LOCATIONAL MARGINAL PRICING

Abhishek Tyagi *
Department of Electrical Engineering
Delhi Technological University
New Delhi, DL 110042
abhishektyagi@dtu.ac.in

Ram Bhagat
Department of Electrical Engineering
Delhi Technological University
New Delhi, DL 110042
bhagat.ram@dtu.ac.in

ABSTRACT

Electric power generation, transmission, and distribution systems are attracting a large amount of interest from researchers with the development of the smart grid technologies. A smart grid aims at effective control and conditioning of the distribution of electricity. Pricing signal based distribution system are seen as one of the novel ways to achieve control in a smart grid. In our work, we propose to use a pricing signal modeled after the locational marginal price in the transmission system to locally provide price data to the users. The formulation and implementation of the distributional locational marginal price (DLMP) are achieved to develop a fair pricing model. The work is further practically implemented to a grid with Electric Vehicles in addition to the conventional load. The increasing popularity of EVs because of their ability to reduce greenhouse gas (GHG) emissions will pose a greater challenge in terms of demand on the power grid. We propose to use the DLMP modeling to alleviate congestion in the power grid and develop an optimal charging schedule for EVs.

***K*eywords** DLMP · Electric Vehicles · Optimizations · Pricing · Resource management

1 Introduction

1.1 Smart Grids

The most important challenge of a power system is to operate itself optimally at the true demand-supply schedule in order to minimise its losses. Historically, power systems have utilised highly controlled supply systems usually from generation grids to manage deviations in the load[1]. However, owing to the recent awareness about climate and environment issues and the spurge in integration of information technology with power systems, "Smart Grid" technologies have started to enter the market. Electric power generation, transmission and distribution systems are attracting a large amount of interest from researchers as well as corporates alike with the development of the smart grid technologies. Smart Grids aim to utilise the extensive information from users to make power systems reliable, efficient and much more environment friendly[2].Smart Grids aim to act as inter-faces between generation system and consumers to coordinate the needs of the users with the capabilities of the generators and optimise the utilisation of resources[1, 2].

The envisioned smart grid aims to have the following features:

- *Integration of Renewable Resources:*Although alternate sources of energy have started penetrating in certain areas, complete implementation of these resources will require a more flexible management system[2]. Smart Grids utilise effective Demand-Side Management(DSM), more efficient use of transmission and intelligent storage to allow for the use of renewable generation in distribution systems. Also, the pricing infrastructure developed is such that it encourages the utilisation of renewable energy over conventional sources.[3]
- *Demand-Side Management*The problems associated with the integration of distributed renewable energy resources is dealt by a lot of researchers but an alternate approach to solving the problem is the involvement of

*

the consumer in the electricity market[4]. Pricing signals can be used as effective methods of control signals and responsive demand allows consumers to decrease their energy response on the basis of the availability of resources[5]. The first one refers to those changes applied by consumers to their electric load profile in response to energy market price signals for improving the economic efficiency of their energy consumption. This model adds to the efficiency of electricity markets by discouraging energy load when the real-time price is high and encouraging it when it is low. Further, this shall reduce the peak demand and make the electricity market more effective. [**?**, 6]

- *Congestion Management:* Smart Grids integrate congestion management from the transmission system to the distribution system as well. Solid State devices such as Flexible AC transmission (FACTS) controllers have been proposed for power flow control[4]. However, dynamic pricing signals can also be used to manage line flow limits during peak hours[7].

The last decade of the 20th century has seen growing concerns been raised regarding energy independence and climate change. Governments and other institutional organisations are working on developing policies to address this issue. The major focus is the consumption of fossil fuels and vehicular emission of green-house gases. In the U.S., the fuel economy standards on auto-mobiles have been set higher numerous times in the past ten years[8]. These concerns over carbon footprints have promoted the development of electric vehicles (EVs) as an alternative to petrol and diesel powered transport[9].Another major attraction for electric vehicles is the large scale integration of renewable energy into the power system. EVs are an attractive option to balance the uncertainties introduced in the system due to renewable energy[10].The number of electric vehicles on the road increased from zero in 1991 to two million in 2010 according to an Energy Foundation study[8]. Consequently, transportation economists have projected that EVs will comprise 64 to 86% of light vehicle sales in the US by 2030[11].

Although it has immense benefits, the large-scale integration of EVs into the power grid poses serious threats towards the stability of the grid. As suggested by Rahman and Shrestha, large scale deployment of EVs will eventually mean increased demand, especially at peak hours, impacting the reliability of the system. Demand patterns inducing flows that exceed the design limits to lead to congestion in the grid. Congestion from EVs can be observed at the medium voltage (MV) level, as demonstrated by a number of studies.[12, 13, 14] Hence, large scale uncoordinated charging of EVs can significantly affect network security[15]. Power quality degradation is also expected from the irregular demands][16]. These factors make it necessary to establish a coordinated standard for charging of EVs. The immense potential for smart grid technology lies in the various opportunities for control and coordination in power systems at the consumer end that have yet not been explored at all. Although a lot of research has been done recently in this regard, most of the research focuses on electronic controllers such as distribution class electronic switches and Solid State Transformers (SST)[17, 18].

In our work, we have developed a pricing infrastructure which can be used as a control feature of the smart grid. These pricing signals in turn will act as control signals to affect demand response, renewable energy penetration and congestion management. We propose to use a pricing signal modelled after the locational marginal price in transmission system to locally provide price data to the users. On a practical scale, we aim to utilise the model developed in Part-1 to develop a price based modelling approach to alleviate congestion induced by electric vehicles. Price based congestion management will ideally operate by the mechanism of generation re dispatch in response to the price signals.

2 Literature Review

Before we move towards developing the model to generate pricing signals, we shall look into the structure of the day-ahead and real-time electricity market and develop the theoretical concept of DLMP.

2.1 Electricity Market

The fact that electricity is a commodity that cannot be stored economically allows for the development of an electricity market place. To facilitate trade among power producers and consumers, an e-commerce marketplace called pool is developed and a framework is made to allow different types of contracts[19]. The market allows short-term trades that deliver electricity for the next day by utilising day-ahead pricing and intra-day markets that deliver electricity in the next 15 minutes[20].

2.2 Real Time Pricing

Throughout a day, there are certain hours that show low demand whereas we observe huge spikes in some places. Real Time price is an electricity rate that fluctuates according to the varying costs and amounts of generation and the demand

from the market. The main aim is to ensure that these real time prices reflect actual wholesale prices at different times of the day and the users are incentivised to shift loads to (o -peak) hours and hence ensure that the (peak-to-average ratio) is reduced[2, 21, 22]. An auction is carried out in the market every hour to calculate the market clearing price and consumption bids are taken from all end users.The concept of spot pricing for utilities was suggested by William Vickrey [23] in 1971.His idea was further developed by Bhon, Caramanis, and Schweppe [24], in 1984. They proposed a model which considered the marginal price of energy, losses, and congestion to determine real time prices. The dynamics of day ahead market is essential as it acts as the base price for the calculation of the real time prices. In a day-ahead market, different prices are quoted for each hour of the next day. The average is then taken to be the average of the day. These prices are considered to be the clearing price for the amount bid at that time. Any deviations from this bid can be bought or sold by the consumer at the real time market clearing price the next day[19, 20].

2.3 Locational Marginal Pricing

The Locational Marginal Price (LMP) represents the marginal cost to supply the next megawatt hour increment in power at the transmission bus without violating any security limits[4]. The LMP is calculated in the transmission system at every node and is calculated every 5 minutes on a real time market. According to Schweppe [25] the locational marginal price represents the truest cost of electricity. The major factors that affect the LMP at a bus are the generator bid prices, the amount of congestion experienced by the transmission system elements and the losses in the system[25]. Unlike the transmission system where nodal pricing is regularly used, distribution systems still make use of at pricing system leading to market inefficiency. Distribution Locational Marginal Price (DLMP) is defined as the real-time cost of providing one extra megawatt of energy at any point on the distribution system [2]. The implementation of such a model in the distribution system would lower total electricity costs for the end-user, mitigate the need to increase line load limits and also act as a perfect support mechanism to allow the utilisation of renewable generation[26, 4].

2.4 Factors Contributing To DLMP

The DLMP at any node is calculated by taking into account the transmission LMP and the distribution objectives and costs. Equation 1 is one of the formulations of DLMP.

$$DLMP = w_1 \sum \pi_i LMP_i + w_2 \sum (|I_k + \delta I_k|^2 - |I_k^2|) r_k + w_3 \sum P_\gamma + w_4 \sum \frac{|I_k|^2}{I_k{}^{\text{rating}}} \tag{1}$$

The DLMP can be broken down into four major components. These include:

- Marginal Energy Cost (MEC): This refers to the cost of energy at each substation and is calculated by the LM Pi at each substation and the contribution i of each substation.
- Marginal Loss Cost (MLC): The 2$^{\text{nd}}$nd term refers to the cost of I^2R losses in the branch k in the power system over an hour.
- Renewable Encouragement Factor: The 3$^{\text{rd}}$ term allows easy implementation of renewable energy and P denotes the cost of renewable generation over one hour.
- Marginal Congestion Cost (MCC): The 4$^{\text{th}}$ applies the penalty for the congestion in the line and penalises for high current loading

2.5 Demand Side Management in EV Charging

Demand Side Management is the modification of consumer demand through various methods such as financial implications to improve service and reduce consumption. Coordinated EV charging can be broadly classified on the basis of the decision making entity into centralized and distributed methods [27]. In case of centralized decision making, there exists large aggregators who manage multiple EVs. The EVs send their availability schedule and battery specifications to the aggregator who, on the basis of its profits [28, 29, 30], EV power costs [**?**], [31],[32] and reducing peak-to-average ratios [33]. On the other hand, in the distributed system, the flow of information is from the aggregator to the EVs who utilise their own understanding of the market to develop its charging plans. A mutual agreement needs to reached among all the parties as each party tries to minimise its individual costs [34] .Various optimisation techniques have been previously utilised in DSM literature to solve energy consumption scheduling problems. These include mixed-integer linear programming as done by Zhang et al. [35], quadratic programming for EV scheduling as done by Vandel et al. [36] and mixedinteger quadratic programming to allow for decentralised demand side management [37]. Most studies concentrate on mitigating the various impacts of EV charging load such as increases in peak load, power losses and decreased voltage.

2.6 Optimal EV Charging Management

Ruoyang Li et al [38] have theoretically developed an aggregator based EV charging management system to mitigate the negative impacts of EV loading on the grid. It considers the EV aggregators to be pro t seeking entities providing charging solutions to the EVs. The EV aggregators are price-takers and do not control the market. It thus proposes to forecast EV demands on the basis of all aggregators minimizing their individual costs whereas the conventional demand will be forecasted according to day-ahead prices. Figure 1 refers to the model developed to alleviate congestion caused

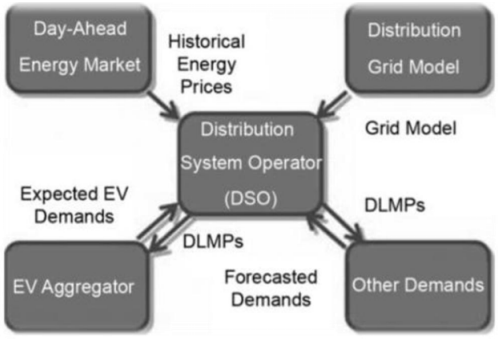

Figure 1: Congestion Alleviation from EVs using DLMPs

by EVs using pricing signals. The problem is solved from the point of view of the Distribution System Operator (DSO) to obtain the optimal solution for each EV aggregator. However, it can be easily proved that the efficient allocation of EV charging ${x_{i,t}}^*$ of the DSO problem is optimal for each EV aggregator under the DLMPs as well. As a corollary, the efficient allocation of the DSO problem ${x_{i,t}}^*, {c_{i,t}}^*$ can be achieved in a decentralized system under the DLMPs.

2.7 Karush-Kuhn-Tucker Conditions

The modelling and problem formulation utilises the Karush-Kuhn-Tucker (KKT) conditions (also known as the KuhnTucker conditions) to achieve optimization solution. First published in 1951 [41], the KKT conditions are first order necessary conditions for a solution in nonlinear programming to be optimal, provided that some regularity conditions are satisfied. KKT is essential in mathematical optimization as it generalises the method of Lagrange multi-pliers by allowing inequality constraints. In general, many optimization algorithms can be interpreted as methods for numerically solving the KKT system of equations. Through literature review, we can see the importance of LMP signals in distribution system and its use as a control signal in power systems. We have analysed the factors affecting the DLMP calculations and developed a formulation that takes care of all objectives and costs. Moreover, a detailed analysis of the demand side management techniques that have been previously used in EV charging specifically discussing different methods of decision making to decide EV charging schedule, has been done. A theoretical algorithm for coordinated EV charging from a centralized as well as decentralized perspective is discussed. In the subsequent chapters, we shall develop an optimisation problem to calculate DLMP and use it as a congestion alleviation tool.

3 Problem Formulation

In this section we'll formulate the problem that we have solved to determine the DLMP in a system. The cost objective function, constraints and it's relationship with DLMP is shown in the upcoming sections. We have utilised the AC-OPF (Optimal Power Flow) model to derive the DLMPs in Part I and DC-OPF model in Part II. The DCOPF is widely used and is considered to be sufficient for LMP calculation due to its computational efficiency and approximation accuracy[39].

3.1 Optimization Problem

In part I, AC-OPF optimization problem has an objective function which is to be minimized, whereas in part II, DC-OPF optimization- problem has an objective function which is to be maximized. These minimization and maximization are subject to constraints - both equality and inequality. To summarize we can write that,

$$\frac{min}{maxF(x)} \tag{2}$$

such that

$$G(x) = 0 \tag{3}$$

$$H(x) = 0 \tag{4}$$

where,
x: vector of dependent variables

3.2 Part 1

3.2.1 Objective Function

As discussed in Section 3.1, $F(x, u)$ is the objective function to be minimized. It is the total cost of energy to supply the demand in the system, given by,

$$F(x) = \sum_{i=1}^{G} LMP_i P_{Gi} + \sum_{i=1}^{DG} C_{DGi} P_{DGi} \tag{5}$$

where,
G : number of grids in the system
DG: number of renewable energy sources in the system
P_{Gi}: power generated by grid i
P_{DGi}: power generated by renewable generator i
LMP_i: price taken by grid i to deliver P_{Gi}
C_{DGi}: price taken by renewable generator to deliever P_{DGi}

3.2.2 Equality Constraints

As discussed in Section 3.1, the optimization problem has certain equality constraints, also known as Power Balance Constraints. They are obtained by balancing the real and reactive power at all the buses in the system, shown as below,

$$\sum_{i \epsilon G_k} P_{Gi} + \sum_{i \epsilon DG_k} P_{DGi} = P_k + f_{pk} \tag{6}$$

$$\sum_{i \epsilon G_k} Q_{Gi} + \sum_{i \epsilon DG_k} Q_{DGi} = Q_k + f_{qk} \tag{7}$$

where,
v_i: voltage at bus i i: angle at bus i G_k: set of grids connected to bus k DG_k: set of renewable generators connected to bus k P_k: real power load at bus k Q_k: reactive power load at bus k f_{pk}: real power owing out of bus k

$$f_{pk} = \sum_{i=1}^{N} v_k v_i (G_{ki} \cos(\theta_k - \theta_i) + B_{ki} (\sin(\theta_k - \theta_i))) \tag{8}$$

f_{qk}: reactive power owing out of bus k

$$f_{qk} = \sum_{i=1}^{N} v_k v_i (G_{ki} \sin(\theta_k - \theta_i) - B_{ki} (\cos(\theta_k - \theta_i))) \tag{9}$$

3.2.3 Inequality Constraints

The network inequality constraints for an AC-OPF optimization problem can be divided in general in three parts:
Line flow limits
There is a constraint in the power owing any two buses i and j i.e S_{ij}, given by

$$0 \leq S_{ij} \leq {S_{ij}}^{\max} \tag{10}$$

where,

$$S_{ij} = \sqrt{P_{ij}^2 + Q_{ij}^2} \tag{11}$$

$$P_{ij} = \frac{[v_i^2 - v_i v_j \cos(\theta_{ij})]r_{ij} + [v_i v_j \sin(\theta_{ij})]x_{ij}}{r_{ij}^2 + x_{ij}^2} \tag{12}$$

$$Q_{ij} = \frac{[v_i^2 - v_i v_j \cos(\theta_{ij})]x_{ij} - [v_i v_j \sin(\theta_{ij})]r_{ij}}{r_{ij}^2 + x_{ij}^2} \tag{13}$$

Voltage Limits
The voltage at all the buses can only vary between a minimum and a maximum value. Hence for any bus k,

$$v_k{}^{\min} \leq v_k \leq v_k{}^{\max} \tag{14}$$

Power Supply Limits
The power supplied by the grid and the renewable generators can also vary only in a given range. Hence for any grid or renewable generator i we can write,

$$P_i{}^{\min} \leq P_i \leq P_i{}^{\max} \tag{15}$$

3.2.4 Calculating DLMP

The optimization problem described in the Section 3.1 can be solved using the Lagrangian multipliers

$$L = F(x,u) + \sum_{k=1}^{N} \lambda_K G_K(x,u) + \sum_{l=1}^{M} \gamma_l H_l(x,u) \tag{16}$$

The DLMP at each bus k is simply the Lagrange multiplier associated with the real power balance constraint for that bus. [43]

$$DLMP_k = \lambda_k \tag{17}$$

3.3 Part II

3.3.1 Objective Function

As discussed in Section 3.1, F (x; u) is the objective function to be minimized. We are solving the problem from the DSO side and the objective is economic allocation for household demand and EV charging energy. Hence, the DSO objective is to maximise the social surplus, which can be mathematically presented as

$$maxF(x,u) \tag{18}$$

$$F(x,u) = \sum_{i \epsilon N} \sum_{t \epsilon T} \int_a^{c_{i,t}} P_{i,t}(\tau_i, t) d\tau_{i,t} - \sum_{t \epsilon T} P_{LMP_t} q_{g,t} \tag{19}$$

where,
N_c: Number of demand nodes
T: Number of hours for which system is analysed
$T_{i,t}$:Demand variable at time t and node i
$P_{i,t}(\tau_i, t)d\tau_{i,t}$: Benefits of using demand

$$P_{LMP_t}$$

: System LMP at time t for the node feeding the grid
$q_{g,t}$: Power supplied by the generator to the grid at t
$c_{i,t}$:Conventional household demand at time t at node i

The objective function consists of two terms. The first one represents the socialvalue of meeting the conventional demand, given by the area under the demand functions. The bene t of EV demand is not used as it is constant as long as the EV demand is met within the day [40]. The second term rep-resents the total cost of satisfying both the conventional

as well as the EV demand.
The optimization function can be further decomposed as follows:

$$F(x,u) = \sum_{i\epsilon N}\sum_{t\epsilon T}\int_{a}^{c_{i,t}} P_{i,t}(\tau_i,t)d\tau_{i,t} - \sum_{t\epsilon T} P_{LMP_t}\sum_{i\epsilon N_c}(c_{i,t}+x_{i,t}) \tag{20}$$

$$= \sum_{i\epsilon N}\sum_{t\epsilon T}\int_{a}^{c_{i,t}} P_{i,t}(\tau_i,t)d\tau_{i,t} - \sum_{t\epsilon T} P_{LMP_t}\sum_{i\epsilon N_c}(c_{i,t}) - \sum_{t\epsilon T} P_{LMP_t}\sum_{i\epsilon N_c} x_{i,t} \tag{21}$$

where,

$$\sum_{i\epsilon N}\sum_{t\epsilon T}\int_{a}^{c_{i,t}} P_{i,t}(\tau_i,t)d\tau_{i,t} - \sum_{t\epsilon T} P_{LMP_t}\sum_{i\epsilon N_c}(c_{i,t}) \tag{22}$$

is the social welfare corresponding to the conventional demand.

$$\sum_{t\epsilon T} P_{LMP_t}\sum_{i\epsilon N_c} x_{i,t} \tag{23}$$

is the EV charging cost.

3.3.2 Equality Constraints

Energy Balance Constraints
The total energy coming into the grid at time t should be same as the energy supplied by the generator. Net active power import/ export at time t for all nodes should be zero.

$$\sum_{i\epsilon N} r_{i,t} = 0 \forall t\epsilon T \tag{24}$$

where,

$$r_{i,t} = c_{i,t} + x_{i,t} \tag{25}$$

here,
$r_{i,t}$ is the net active power import/ export at time t at node i

Generation Node Balance Constraint
In this constraint the $r_{i,t}$ of the generator is made equal to the power supplied by the generator to the grid. Mathematically,

$$r_{g,t} + q_{g,t} = 0 \forall t\epsilon T \tag{26}$$

3.3.3 Inequality Constraints

Transmission Balance Constraint
There is a limit on the power that can flow in each line and hence the constraint is represented as,

$$-K_l \leq \sum_{i\epsilon N} D_{l,i} r_{i,t} \leq K_l \forall t\epsilon T, \forall l\epsilon L \tag{27}$$

where,
K_l: MVA capacity of line l
$D_{l,i}$: Power Transfer Distribution Factor (PTDF) coefficient of line l with respect to a unit injected at node i PTDF can be calculated as follows,

$$PTDF = diag(B) * A_r * (A_r{}^{\mathrm{T}} * diag(B) * A_r)^{-1} \tag{28}$$

here,

$$B = AX^1A^T \tag{29}$$

A: branch-to-node incidence matrix
X: diagonal reactance matrix
A_r: reduced incidence matrix

Charging Energy Limit Constraints
There is a limit on the maximum energy that a EV can take at one time from a charging station

$$0 \leq x_{i,t} \leq E_{i,t} \tag{30}$$

where,
$E_{i,t}$: EV battery size

Driving Requirement Constraints
The SOC (State of Charge) of EV batteries at time t for EV i is the sum of its initial SOC and total charging energy up to time period t-1 minus the total driving energy requirement up to time t.

$$S_{i,t^{`}} \leq S_{i,0} + \sum_{t^{`} \leq t-i} x_{i,t^{`}} - \sum t^{`} \leq td_{i,t^{`}} \leq S_{i,t^{`}} \forall i \epsilon N_c, \forall t \epsilon T - 1 \tag{31}$$

where,
$D_{i,t}$: distance travelled at time t by

3.3.4 Calculating DLMP

The DLMP for all the nodes in the system can be calculated by using the KKT multipliers found by solving the optimization problem defined in 3.4.1 using the constraints defined in 3.4.2 and 3.4.2.

$$DLMP = \begin{cases} -\mu^+_{i,t} + \mu^-_{i,t} - \sum_{t^{`} \leq t+1} K^+_{i,t^{`}} + \sum_{t^{`} \leq t+1} K^-_{i,t^{`}} & \forall_i \epsilon N_c . \forall_t \epsilon T - |T| \\ -\mu^+_{i,t} + \mu^-_{i,t} & \forall_t \epsilon |T| \end{cases}$$

We have theoretically formulated the optimization problem with the objective function and the constraints which were solved to gives us the DLMP at each bus. In the next chapter we will show how this theoretical approach can be modelled in software and can be utilised for calculation of DLMP in practical systems.

4 Modelling

4.1 Introduction

In the previous chapter in Section 3.2 we theoretically formed the optimization problem that needs to be solved to obtain the DLMP. This chapter deals with creating a model in MATLAB that solves the optimization problem and calculates the DLMP.

4.2 Non-Linear Programming Function MATLAB

We have used the MATLAB function $fmincon$ to solve the optimisation problem. $fmincon$ is a non-linear programming solver which gives the minimum of a function with respect to constraints.

$$minf(x)suchthat = \begin{cases} c(x) & \leq 0 \\ c_{eq}(x) & = 0 \\ A_{eq}.x = B_{eq} & \\ lb \leq x \leq ub & \end{cases}$$

Table 1: 12 Bus Distribution System Data

Voltage Base(kV)	V_B=2
MVA Base (MVA)	S_B=1
Feeder Impedance	z = 0.896+j0.7743
Feeder Length(mile)	L=0.5
Feeder Thermal Limit	I_{max} = 240A

4.3 Cost Function

We have used a separate function $myfun$ which returns the total cost of the energy summing the cost of energy supplied by each generator. We have used cost functions of two types in our analysis:

4.3.1 Polynomial Cost Function

The fuel cost function for grids or conventional thermal generators is represented by a quadratic polynomial function [44] given as,

$$C_i(P_{G_i}) = a_i + b_i P_{Gi} + c_i P_{G_i}^2 \tag{32}$$

4.3.2 Linear Cost Function

The cost for renewable energy is taken to be linear. It is assumed to contain the investment costs of equipments and the operation and management cost of generated energy. The cost function for renewable energy is hence given as

$$C_i(P_{GD_i}) = m_i P_{G_i} \tag{33}$$

Where, m_i is the slope of the assumed linear cost function.

4.4 Constraints

There are two types of constraints, equality and inequality. These constraints can be further divided as linear or non linear.

Linear Constraints
The voltage limits and power generation limits are linear.

Non-Linear Constraints
The power balance equations and Line flow limits are non linear constraints.

Having summarised the method in which we have modelled the DLMP in the software MATLAB, in the coming two chapters we'll consider a sample system of 12 buses, define its specifications and discuss the results of various cases on it.

5 System Specifications

In the previous section we have discussed modelling of the optimization problem in MATLAB. We shall utilise the model for two different systems. Firstly, a 12 bus system is studied to calculate DLMP across the system. Secondly, a part of the bus 4 distribution system of RBTS is used to demonstrate the efficacy of DLMP signals as an effective tool to alleviate congestion from EV demand. This chapter deals with the specifications of both the systems and the discusses the data selected for each case

5.1 Part-I

5.1.1 Elements and Circuit Diagram

The sample system we have considered is a 12 bus system as shown in Figure 2[4].

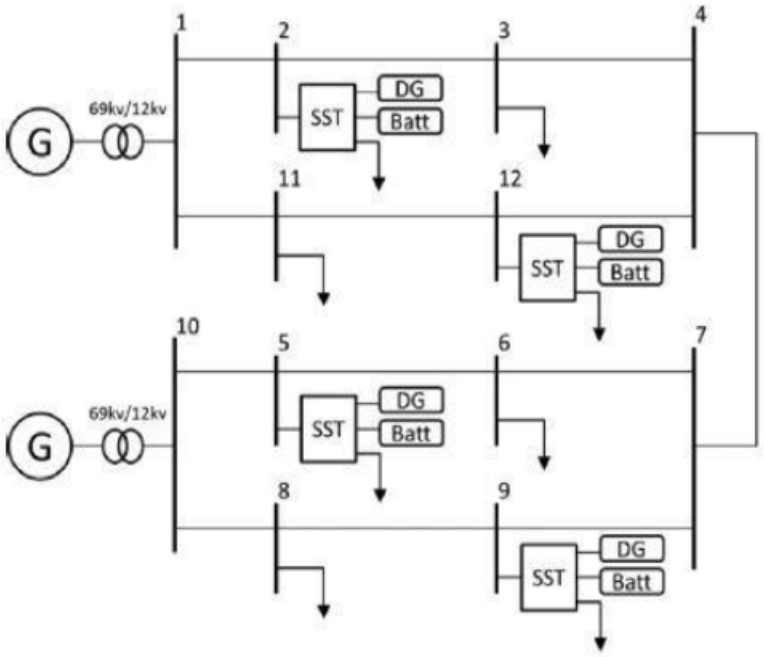

Figure 2: 12 Bus Distribution System

Table 2: Coefficients for Cost of Grid

Bus Number	$a_i(^{Rs.}/_{hr})$	$b_i(^{Rs.}/_{MWhr})$	$c_i(^{Rs.}/_{MW^2hr})$
1	0	3.00	0.00250
10	0	2.75	0.00625

Generators
It has two grids connected to bus 1 and 10. Four renewable generators are connected to buses 2, 5, 9 and 12. We have taken the renewable energy to be wind energy.

Loads
There are loads connected to buses 2, 3, 5, 6, 8, 9, 11 and 12, whose values are decided by the load profiles shown in Figure 6 in Section 6.2 for different cases.

Other Specifications of the Distribution System
Some other specifications of the system like base units and feeder impedance are shown in the Table 1.

5.1.2 Cost Funtions

As discussed in Section 4.3 the costs are of two types.
Grids
The cost of grids is taken to be quadratic polynomial and the coefficients a_i, b_i and c_i for the same are tabulated in Table 2[40]

Renewable Wind Generators
The cost of the renewable wind generators is taken as linear passing through origin and the slope for the same is tabulated in the Table 3. [40]

Penalty in Real Time
In the day ahead market power from the grids as well as the wind generators are decided based on the forecasted load.

Table 3: Coefficients for Cost of Renewable Generators

Bus Number	$m_i(^{Rs.}/_{MWhr})$
2	3.25
5	3.5
9	3.25
12	3.5

Table 4: Connection Line Types

Line Type	Line Length	Line Number
1	0.6	2 6 10 14
2	0.75	1 4 7 9 12
3	0.8	3 5 8 11 13

But since in the real time market the actual load differs from the forecasted load, some extra power is drawn from either the grid or the wind generators. The grid in real time imposes a penalty i.e. charges a high price if more than scheduled load is drawn. In such a case getting power from the wind generators become cheaper. But there is a limit on the power generated by the wind generator (Section 3.4.3), so when its maximum is reached, the system is forced to draw power from the generator leading to an increase in the cost.

5.2 Part-II

5.2.1 System Outline

A sub part of the Bus 4 distribution network of the RBTS system is used as a case study to test the model.

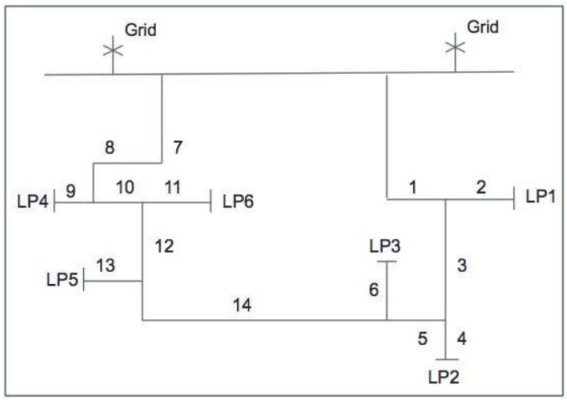

Figure 3: Single Line Diagram of test system

Figure 3 [40] shows the single line diagram of the test system. The system has 2 supply points, 6 load points and 2 EV aggregators (each consisting of 25 EVs under its ambit). The electric distribution systems of RBTS represent typical distribution networks and follow the general principles and practices regarding topology and ratings. Table 4 lists the different types of lines along with respective line lengths.

Customer Data
The customer data consists of peak and average loads for each load point. The inverse demand function at each bus is assumed to be linear with a price elasticity of 0.1 as shown in Figure 4. This level of demand price elasticity is consistent with empirical studies.

EV
Table 6 summarises the EV data. The battery size of each EV varies according to EV driving requirements. It is assumed that the maximum charging power is 1.15 kW (based on a 5 A, 230 V connection). The energy consumption while

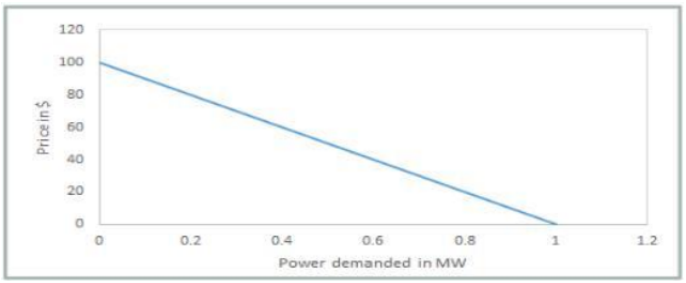

Figure 4: Demand Curve of each Load

Table 5: Customer Level Data

Load Points	Average Load/LP (MW)	Peak Load/LP(MW)
1,3,4,5	1.0	1.63
2,6	1.5	2.445

driving is kept at 0.15 kWh/km. The EV battery can fluctuate between a maximum SOC of 85% and a minimum of 20%. Each EV has an individual initial SOC that is chosen according to its driving schedule.

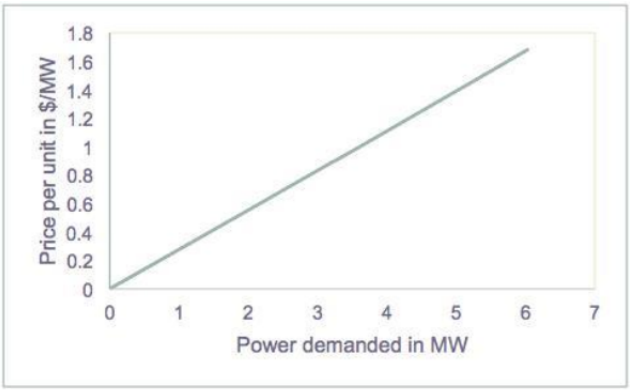

Figure 5: Generator Cost Curve

Generator Cost Function
The generator cost function is defined as a quadratic polynomial represented by the equation

$$P = 0.275Q + 0.0006250Q^2 \tag{34}$$

where Q is the energy demand and P is the cost Figure 5 shows the graph of the generator cost with the net energy demand.

In this section we have defined the system specifications, limits and cost functions. Using these values in the model (Section 4) we'll run different cases which will be discussed in the next Section.

6 Results and Discussions

This section is divided in two parts - Part I and Part II. For each part we first present the data that is used as input for the system and then we discuss the observations and conclusions for different scenarios.

6.1 Part-I

In this section we shall discuss the following scenarios:

- Day ahead market

Table 6: EV Data Summary

EV Parameter	Value
EV Battery Size	25 kWh
Energy Consumption of Driving	0.15kWh/km
Minimum SOC	20%
Maximum SOC	80%

- Real time market
- Real time market with responsive loads
- Real time market with congestion

6.1.1 Data Used

To get the day-ahead pricing signal, we shall use the forecast of the load for 24 hours as shown in Figure 6 [48] and the forecast of the wind energy production, as shown in

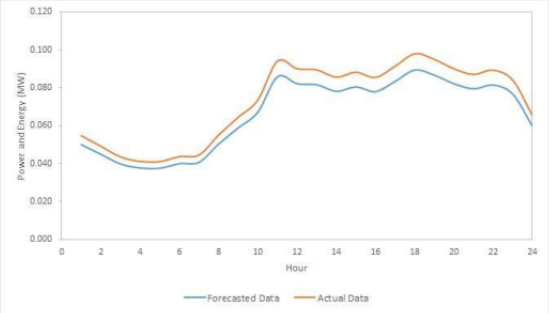

Figure 6: Load Profile-Forecast and Actual

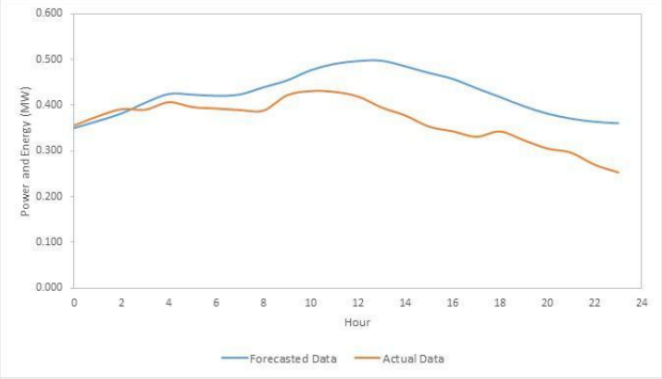

Figure 7: Wind Power Generation Profile-Forecast and Actual

6.1.2 Results

Day ahead market As discussed in Section 2.1.2, the bidding for the day ahead market happens 24 hours prior to the day when the actual requirement occurs. Since the actual load profile and wind power generation data is not available, we use the forecasted data to predict the production bills by all renewable generators as well as the grid.

Figure 8 shows a comparison of the Total Load, total contribution from both the grids and the renewable sources and the value of the total cost function over the period of 24 hours. From Figure 8, it can be observed that as the total load in the system increases, the total cost as well as the contribution of wind energy increases. However the contribution of

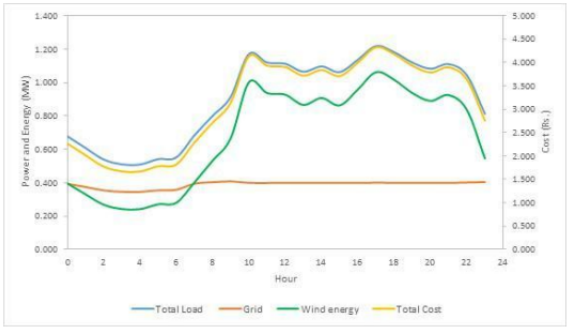

Figure 8: Day Ahead: Comparison of load, generation cost over 24 hours

grid remains almost the same. This is beneficial for the system as the renewable sources are able to take care of load variations and we do not have to retrieve extra energy from the grid. The grid supplies up to a predefined rate at a price which is cheaper than renewable sources as discussed in 5.2.2. After that level, it is cheaper to take from the DGs, in order to promote these sources of energy.

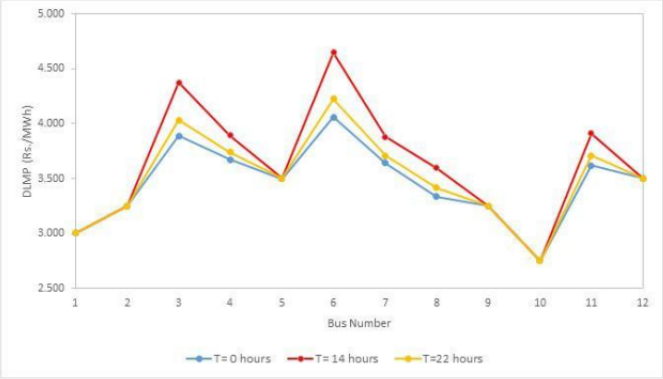

Figure 9: Day Ahead Market: Comparison of DLMP at different times

Figure 9 shows the variation in DLMP at different hours of the day for all the buses. It is very interesting to see that the DLMP is highest at t=14 hours which is a peak load hour and lowest at t=0 hours which is an off peak hour. Hence, it will provide an added incentive to the end-user to shift his loads to o-peak hours. The DLMP at buses 1, 2, 5, 9, 10

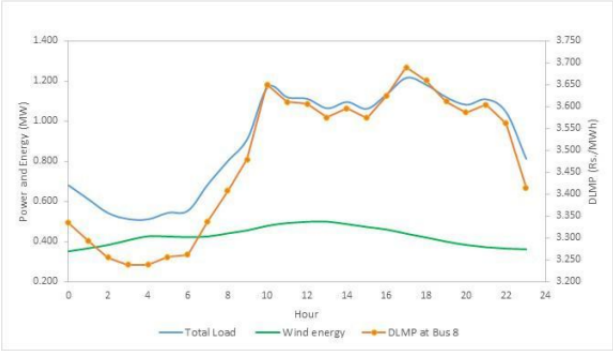

Figure 10: Day Ahead: Variation in DLMP with load and wind generation

and 12 are lower as compared to the other buses. This is because at these buses we either have a grid or a wind power generator. Since in supplying the loads at these buses the line loss component of DLMP doesn't come into picture, the DLMP is significantly less. Figure 10 is highlights the variations in DLMP with the changing load and wind generation

pro les at bus 8. An increase in the DLMP is seen with the increasing load as is expected. Further, when the generation is less, an increase in the DLMP is observed.

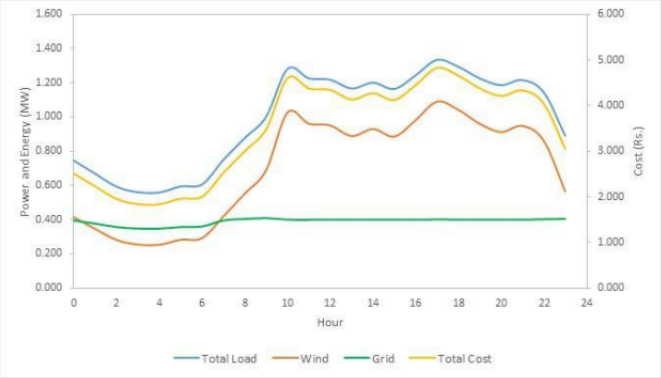

Figure 11: Real Time: Comparison of the load generation cost over 24 hours

Real Time Market

In the real-time market, the bidding is usually done 15 minutes before the energy is required at the load. At this moment, we have actual data relating to the load requirements at all buses and the generation by the renewable sources and hence that is used. The load usually shows a positive diversion from the forecast and is higher. It is this difference in load that has to be auctioned to the production companies. Also, the actual generation by renewable sources might be less as compared to the forecast and in case if the day-ahead bid amount is not produced on one of the buses, the concerned generator has to buy it from other sources.

Figure 11 shows a comparison of the Total Load, total contribution from both the grid and the renewable sources and

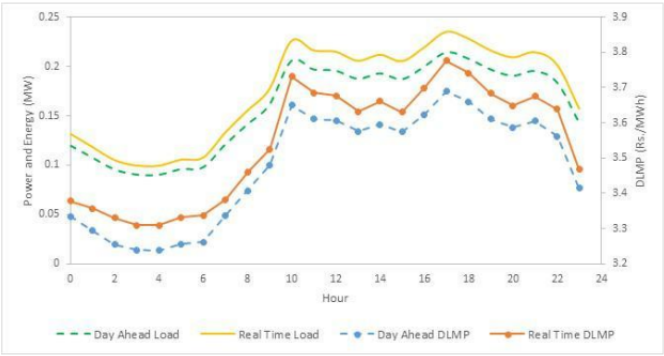

Figure 12: Comparison of DLMP and Load for Real Time and Day Ahead

the value of the total cost function over the period of 24 hours in the real time market. The trends followed are similar to Figure 8.

As the load requirements in the real time increase as compared to the day ahead case, the DLMP signals also show a spurge. This is seen in Figure 12. Hence, an added penalty is applied to the loads that divert from the initially bid amount making the process of buying electricity in the real time market expensive. This makes economic sense as well since if there is a load in urgent need of electricity, the price charged can be increased. It is also seen that the change in DLMP is proportional to the change in the load. If major diversions from the initial bid are made, the DLMP will shoot up.Also, as in the day ahead case, the DLMP shows spikes in value when the load increases on the corresponding bus. This behaviour is seen in Figure 13 for the case of bus 8 and can be a major deterrent for peak loading by different consumers.

Real time market with responsive loads

The results for the real time indicate that all the buses are at their maximum loads with Bus 6 having the highest DLMP of 5.21 as well as the maximum load of 0.23 MW. In a responsive system, the load should ideally adjust its consumption with respect to the price signal. The load at Bus 6 is made responsive to see the effect of demand response. It can adjust its load from the maximum value of 0.23MW to 0 MW.

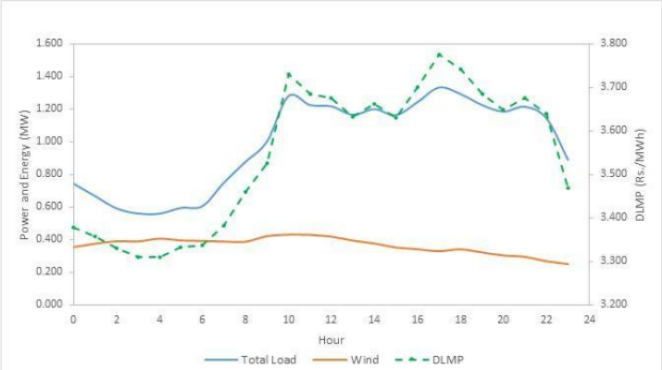

Figure 13: Real Time: Variation in DLMP with load and wind generation

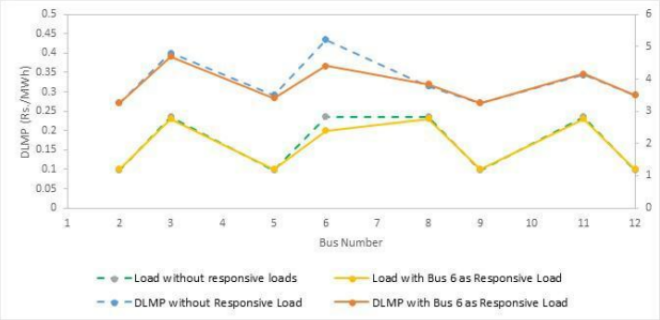

Figure 14: Addition of Responsive Load: Effect on DLMP and Load

The results of the test shows clear instance of demand response. When the load at Bus 6 is made responsive, it responds by reducing its consumption to 0.20 MW. The DLMP at Bus 6 also goes down to 4.40 from 5.21 indicating adequate amount of responsivity in the demand. Hence, we can reduce the demand in peak hours as well (peak-to-average ratio) by implementing demand response in smart grid systems.

Real time market with congestion
In the real time, the power owing in branch between buses 11-12 was seen to be the maximum. Line limits on this branch are changed to 0.1 MW from 3.2 MW to induce congestion on this line. The AC OPF solution illustrates that the injection from the generator at bus 12 decreases as it will no longer be able to supply to bus 11. As a result, the DLMP at Bus 11 sees a spike and goes upto a maximum value of 5.94.Practically this is because the load at Bus 11 cannot take power either from Bus 12 due to the line congestion limit and will have to look upto Bus 0 or Bus 2 for its load requirements. Since, this is an added pressure and will also incur additional losses, DLMP shows a sharp increase in value.

Driving Data
The driving data used in the model is from the Danish National Travel Survey [13]. The Danish driving data were chosen because the driving behavior in Denmark could be representative of the EV users driving pattern. In Denmark, the average driving distance is about 40 km per day. Customers who need to drive a longer distance might not choose to use EVs. To get the profile of driving pattern for the EV customers in our model we assumed a total of 50 EVs. Then using Table A.11 we get the number of EVs travelling a distance of 0-10km, 10-20km and so on every day. Using the EV availability curve from [40], we divide the distance of each EV travels equally among the hours that it is available for travelling. We eventually combined the first 25 EVs under one EV aggregator and the last 25 EVs under the 2nd EV aggregtor.Figure 17 shows the sample EV availability for an EV. At the times which are marked black the EV is travelling and hence cannot be charged but for the times for which it is shown white it is available for charging.

6.1.3 Case-I

Case I represents the most basic case with 2 EV aggregators and the system at 100% EV penetration. Figure 17 and Figure 18 shows the availability of both EV aggregators for this case. Figure 19 depicts the distance travelled by each

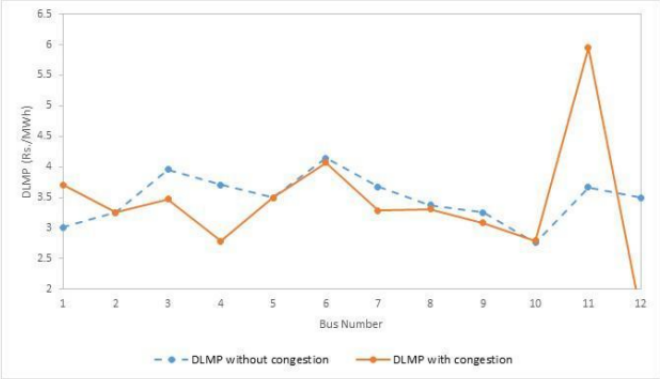

Figure 15: Congestion: Effect on DLMP

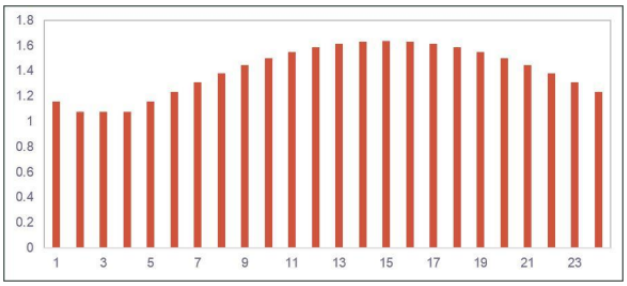

Figure 16: Conventional Customers Demand Curve

Figure 17: Availability curve for EV1

EV at every hour when it is on duty. The results of Case Study I are shown in Figure 20-Figure 22. The day begins with

Figure 18: Availability curve for EV2

an initial EV charge of 25%. Figs 6.16 and 6.17 illustrate the use of DLMPs in reducing the impact of EV loads on the grid at any particular hour. Comparing Figure 21 with Figure 20, we see that EV loads are spread out across multiple hours according to the LMPs at each hour instead of charging at any one hour. This is because charging at one hour would lead to a serious spike in the value of DLMP at that hour and therefore leading to instability in the system. As seen, the EVs charge at times with minimum conventional demand so as to minimize their charging costs and maximize social welfare.

6.1.4 Case-II

Case II represents a case with 2 EV aggregators and the system at 100% EV penetration. Figure 17 and Figure 18 shows the availability of both EV aggregators for this case. In both cases the availability is such that it necessitates that the EVs charge during the high price hours. Figure 19 depicts the distance travelled by each EV at every hour when it is on duty. The driving schedule of each EV.The results of Case Study II are shown in Figure 20-Figure 22. The difference in Case II with respect to Case I is evident from Figure 26 and Figure 27. The EV availability schedule is such that the

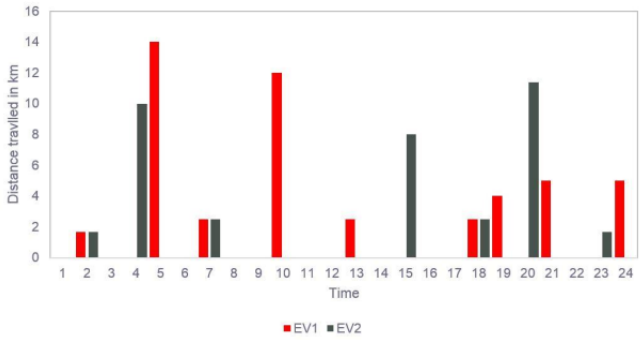

Figure 19: Distance travelled by both EVs across 24 hours

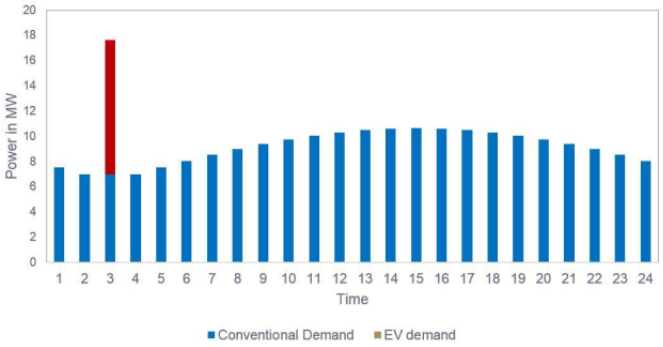

Figure 20: Line 1 loading without DLMPs in Case I

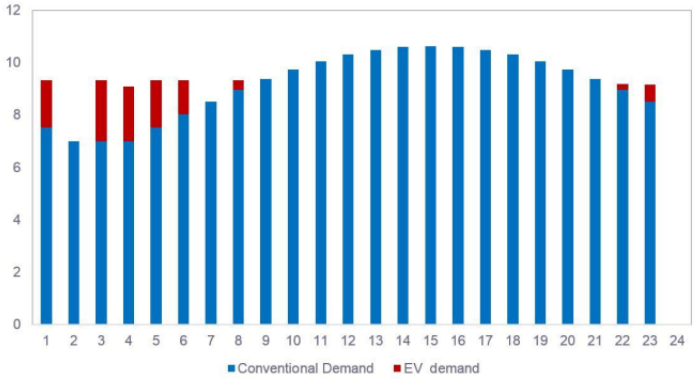

Figure 21: Line 1 loading with DLMPs in Case I

EVs are forced to charge in hours 12, 13 and 14 when the LMPs are generally high. However, even in this case the charging is balanced rather than concentrated at one particular hour.

6.1.5 Case-III

Case III represents a system which has 500% EV penetration in terms of the net EV demand. **??** and Figure 29 illustrate the results for the case. The essential point in this case is the EV loading after DLMPs are used in the system. We see an optimized distribution of EV loading across the 24 hours such as the hours that have low LMP see higher EV load as compared to hours that have high LMP. This is almost constant across time except for hours when the EVs are driving. This ultimately leads to an approximately equitable demand at each hour for the system and hence means a general stability of the system.

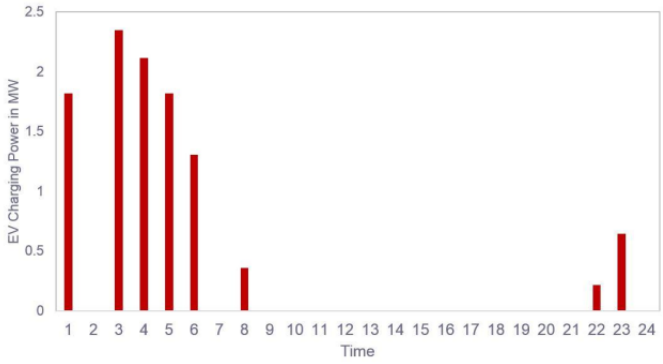

Figure 22: Total EV loads with DLMPs in Case I

Figure 23: Availability curve for EV1 for Case II

Figure 24: Availability curve for EV2 for Case II

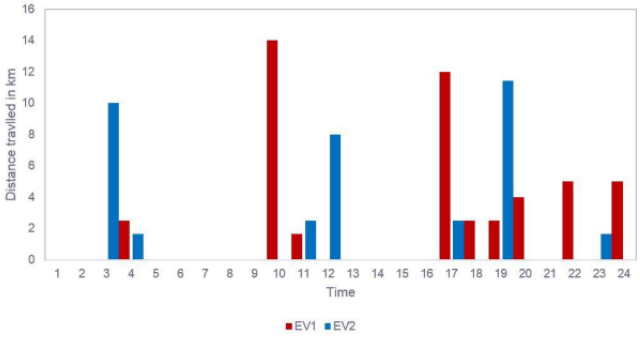

Figure 25: Distance travelled by both EVs across 24 hours for Case II

6.1.6 Case-IV

Case IV consists of the same system as in Case I but with congestion induced in the line 14 by reducing the limits of the line. Figure 30 and Figure 31 represent the results achieved. As a result of the congestion in the system, there is a visible change in the power used to charge the EVs at time 4 when the systems meets the limits.

Fig 6.27 depicts a comparison between the EV demand with and without congestion. The induced congestion is at time 4.As a result this EV charging at time 4 is reduced and in turn compensated at other times of the day.

Figure 32 represents the variation of DLMP and LMP with time at node 11. The DLMP follows the LMP at all times except at time 4 when congestion is induced into the system. This is because the system is lossless system and the distribution price is same as the transmission price. However, at time t=4, congestion in the adjoining line causes a spurt in price of demand indicating a model that discourages users to charge at times when the load is high and shift load accordingly to other hours.

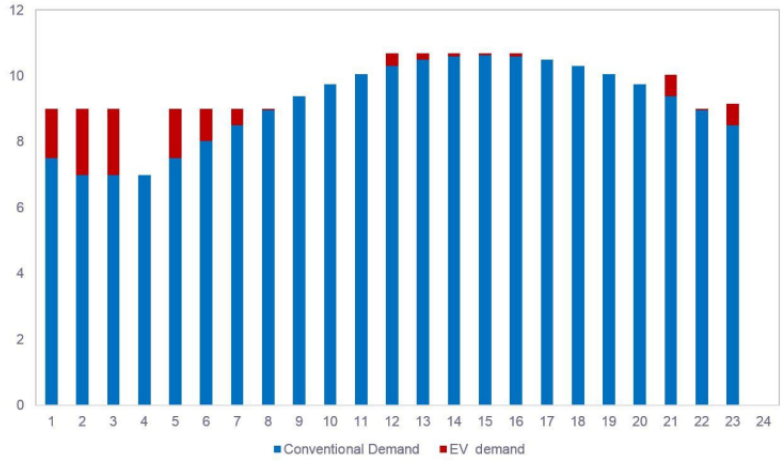

Figure 26: Line 1 loading with DLMPs in Case II

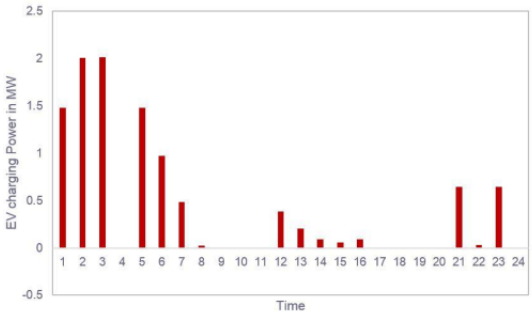

Figure 27: Total EV loads with DLMPs in Case II

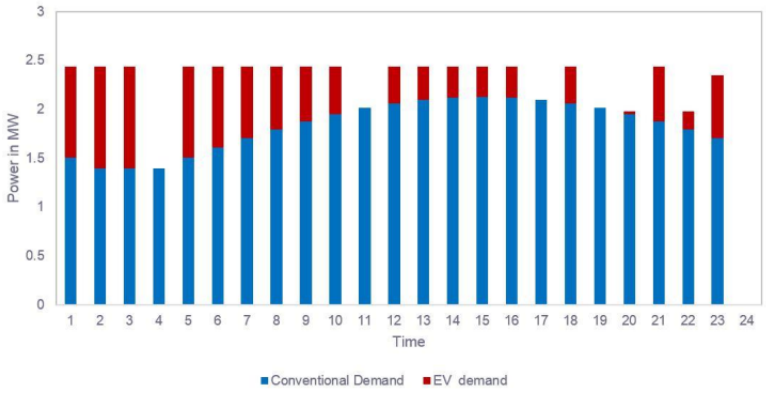

Figure 28: Line 1 loading with DLMPs in Case III

7 Conclusion

This work has two main conclusions. One of the main conclusion of this work is the development of a pricing signal modelled on the lines of Locational Marginal Pricing (LMP) in distribution systems as a control signal. A multi objective optimisation function has been developed for the calculation of the pricing signal. The implementation of the optimisation was developed in MATLAB and a robust model has been developed for the same. Various control objectives such as reduction in cost of energy, reduction of demand in peak hours, improvement of (peak-to-average ratio) and controlled flow in selected lines was successfully achieved. Secondly, a real-life practical implementation of the model is developed for a system with Electric Vehicle based loads in addition to the conventional household demand.

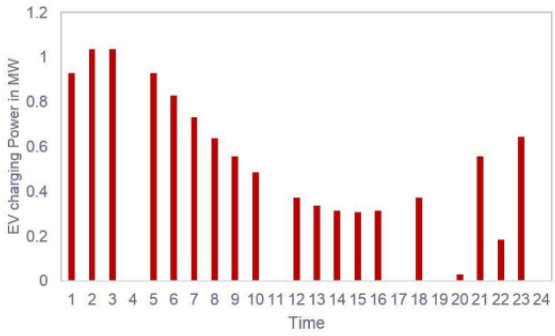

Figure 29: Total EV loads with DLMPs in Case III

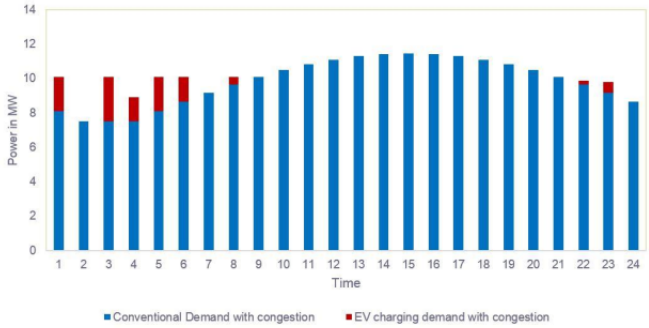

Figure 30: Line 1 loading with DLMPs in Case IV

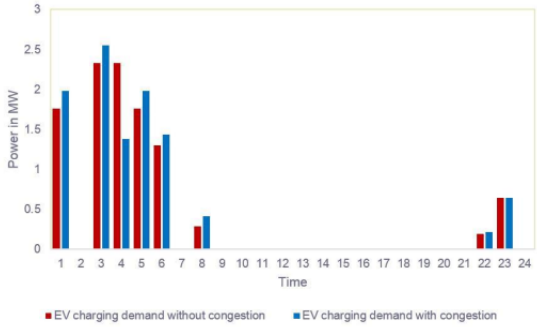

Figure 31: Comparison between EV loads with and without congestion

The model is developed with the aim to mitigate the risks that the grid might face due to large scale integration of EVs. Again,a non-linear constrained optimization schedule is developed and tested on a part of the Bus 4 RBTS system. The model is seen to have successfully alleviated congestion and can be used as a tool for demand side management and EV charge scheduling.

8 Future Work

The demand response shows interesting results and can be practically used to reduce peak power demand. The modelling can be used as a suitable benchmark for the study and development of distribution systems in the future smart grid. The future work requires further development of the model, introduction of other control objectives and testing the model on real-time cases. A well developed pricing infrastructure has the potential to work as a competent control mechanism for the future smart grid.
For the part II of the model, immense scope lies in adding additional feature of spatial optimization across different

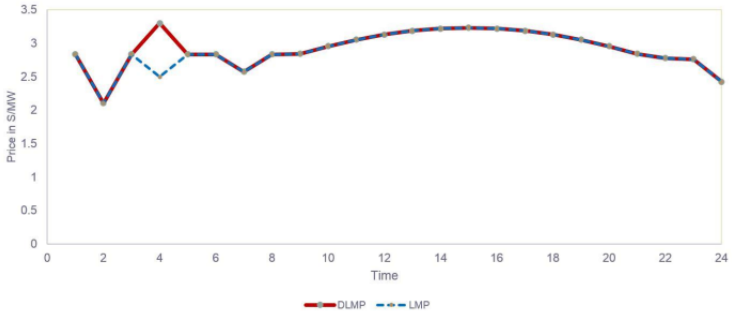

Figure 32: DLMPs at node 11 in Case III

charging stations. We can modify the system to allow EV users to drive to a different station to specifically charge. Further, a higher degree of precision can be achieved by including practical features such as driving distance, opportunity cost of driving time and spatial difference in EV charging costs. We can also expand the system to a multitude of EV aggregators. Further, the system can be expanded to a micro level by expanding the optimization to individual EV aggregators as well.

References

[1] C. W. Potter, A. Archambault, and K. Westrick. Building a smarter smart grid through better renewable energy information. In *2009 IEEE/PES Power Systems Conference and Exposition*, pages 1–5, March 2009.

[2] F. Sahriatzadeh, P. Nirbhavane, and A. K. Srivastava. Locational marginal price for distribution system considering demand response. In *2012 North American Power Symposium (NAPS)*, pages 1–5, Sep. 2012.

[3] G. T. Heydt, B. H. Chowdhury, M. L. Crow, D. Haughton, B. D. Kiefer, F. Meng, and B. R. Sathyanarayana. Pricing and control in the next generation power distribution system. *IEEE Transactions on Smart Grid*, 3(2):907–914, June 2012.

[4] C. Cecati, C. Citro, and P. Siano. Combined operations of renewable energy systems and responsive demand in a smart grid. *IEEE Transactions on Sustainable Energy*, 2(4):468–476, Oct 2011.

[5] A. J. Roscoe and G. Ault. Supporting high penetrations of renewable generation via implementation of real-time electricity pricing and demand response. *IET Renewable Power Generation*, 4(4):369–382, July 2010.

[6] C. Ibars, M. Navarro, and L. Giupponi. Distributed demand management in smart grid with a congestion game. In *2010 First IEEE International Conference on Smart Grid Communications*, pages 495–500, Oct 2010.

[7] P. Zhang, K. Qian, C. Zhou, B. G. Stewart, and D. M. Hepburn. A methodology for optimization of power systems demand due to electric vehicle charging load. *IEEE Transactions on Power Systems*, 27(3):1628–1636, Aug 2012.

[8] Q. Wu, A. H. Nielsen, J. Ostergaard, S. T. Cha, F. Marra, Y. Chen, and C. Træholt. Driving pattern analysis for electric vehicle (ev) grid integration study. In *2010 IEEE PES Innovative Smart Grid Technologies Conference Europe (ISGT Europe)*, pages 1–6, Oct 2010.

[9] Thomas A Becker, Ikhlaq Sidhu, and Burghardt Tenderich. Electric vehicles in the united states: a new model with forecasts to 2030. *Center for Entrepreneurship and Technology, University of California, Berkeley*, 24, 2009.

[10] K. Clement-Nyns, E. Haesen, and J. Driesen. The impact of charging plug-in hybrid electric vehicles on a residential distribution grid. *IEEE Transactions on Power Systems*, 25(1):371–380, Feb 2010.

[11] K. J. Dyke, N. Schofield, and M. Barnes. The impact of transport electrification on electrical networks. *IEEE Transactions on Industrial Electronics*, 57(12):3917–3926, Dec 2010.

[12] L. Pieltain Fernández, T. Gomez San Roman, R. Cossent, C. Mateo Domingo, and P. Frías. Assessment of the impact of plug-in electric vehicles on distribution networks. *IEEE Transactions on Power Systems*, 26(1):206–213, Feb 2011.

[13] M. K. Gray and W. G. Morsi. Power quality assessment in distribution systems embedded with plug-in hybrid and battery electric vehicles. *IEEE Transactions on Power Systems*, 30(2):663–671, March 2015.

[14] S. Bhattacharya, T. Zhao, G. Wang, S. Dutta, S. Baek, Y. Du, B. Parkhideh, X. Zhou, and A. Q. Huang. Design and development of generation-i silicon based solid state transformer. In *2010 Twenty-Fifth Annual IEEE Applied Power Electronics Conference and Exposition (APEC)*, pages 1666–1673, Feb 2010.

[15] A. Mohsenian-Rad and A. Leon-Garcia. Optimal residential load control with price prediction in real-time electricity pricing environments. *IEEE Transactions on Smart Grid*, 1(2):120–133, Sep. 2010.

[16] Ronald Huisman, Christian Huurman, and Ronald Mahieu. Hourly electricity prices in day-ahead markets. *Energy Economics*, 29(2):240–248, 2007.

[17] F. J. Nogales, J. Contreras, A. J. Conejo, and R. Espinola. Forecasting next-day electricity prices by time series models. *IEEE Transactions on Power Systems*, 17(2):342–348, May 2002.

[18] M. Fahrioglu and F. L. Alvarado. Designing incentive compatible contracts for effective demand management. *IEEE Transactions on Power Systems*, 15(4):1255–1260, Nov 2000.

[19] William Vickrey. Responsive pricing of public utility services. *The Bell Journal of Economics and Management Science*, 2(1):337–346, 1971.

[20] Roger E Bohn, Michael C Caramanis, and Fred C Schweppe. Optimal pricing in electrical networks over space and time. *The Rand Journal of Economics*, pages 360–376, 1984.

[21] Jim Frame. Locational marginal pricing. In *2001 IEEE Power Engineering Society Winter Meeting. Conference Proceedings (Cat. No. 01CH37194)*, volume 1, pages 377–vol. IEEE, 2001.

[22] Stephen P. Holland and Erin T. Mansur. The short-run effects of time-varying prices in competitive electricity markets. *The Energy Journal*, 27(4):127–155, 2006.

[23] James JQ Yu, Junhao Lin, Albert Lam, and Victor OK Li. Coordinated electric vehicle charging control with aggregator power trading and indirect load control. *arXiv preprint arXiv:1508.00663*, 2015.

[24] S. Han, S. Han, and K. Sezaki. Development of an optimal vehicle-to-grid aggregator for frequency regulation. *IEEE Transactions on Smart Grid*, 1(1):65–72, June 2010.

[25] E. Sortomme and M. A. El-Sharkawi. Optimal charging strategies for unidirectional vehicle-to-grid. *IEEE Transactions on Smart Grid*, 2(1):131–138, March 2011.

[26] M. Ş. Kuran, A. Carneiro Viana, L. Iannone, D. Kofman, G. Mermoud, and J. P. Vasseur. A smart parking lot management system for scheduling the recharging of electric vehicles. *IEEE Transactions on Smart Grid*, 6(6):2942–2953, Nov 2015.

[27] M. H. K. Tushar, C. Assi, M. Maier, and M. F. Uddin. Smart microgrids: Optimal joint scheduling for electric vehicles and home appliances. *IEEE Transactions on Smart Grid*, 5(1):239–250, Jan 2014.

[28] D. Wu, D. C. Aliprantis, and L. Ying. Load scheduling and dispatch for aggregators of plug-in electric vehicles. *IEEE Transactions on Smart Grid*, 3(1):368–376, March 2012.

[29] D. T. Nguyen and L. B. Le. Joint optimization of electric vehicle and home energy scheduling considering user comfort preference. *IEEE Transactions on Smart Grid*, 5(1):188–199, Jan 2014.

[30] J. de Hoog, T. Alpcan, M. Brazil, D. A. Thomas, and I. Mareels. Optimal charging of electric vehicles taking distribution network constraints into account. *IEEE Transactions on Power Systems*, 30(1):365–375, Jan 2015.

[31] Di Zhang, Lazaros G Papageorgiou, Nouri J Samsatli, and Nilay Shah. Optimal scheduling of smart homes energy consumption with microgrid. In *PROCEEDINGS OF THE FIRST INTERNATIONAL CONFERENCE ON SMART GRIDS, GREEN COMMUNICATIONS AND IT ENERGY-AWARE TECHNOLOGIES (ENERGY 2011)*, pages 70–75. IARIA XPS PRESS, 2011.

[32] Y. Mou, H. Xing, Z. Lin, and M. Fu. Decentralized optimal demand-side management for phev charging in a smart grid. *IEEE Transactions on Smart Grid*, 6(2):726–736, March 2015.

[33] Sarvapali D Ramchurn, Perukrishnen Vytelingum, Alex Rogers, and Nick Jennings. Agent-based control for decentralised demand side management in the smart grid. In *The 10th International Conference on Autonomous Agents and Multiagent Systems-Volume 1*, pages 5–12. International Foundation for Autonomous Agents and Multiagent Systems, 2011.

[34] R. Li, Q. Wu, and S. S. Oren. Distribution locational marginal pricing for optimal electric vehicle charging management. *IEEE Transactions on Power Systems*, 29(1):203–211, Jan 2014.

[35] H. W. Kuhn and A. W. Tucker. Nonlinear programming. In *Proceedings of the Second Berkeley Symposium on Mathematical Statistics and Probability*, pages 481–492, Berkeley, Calif., 1951. University of California Press.

[36] F. Li and R. Bo. Dcopf-based lmp simulation: Algorithm, comparison with acopf, and sensitivity. *IEEE Transactions on Power Systems*, 22(4):1475–1485, Nov 2007.

[37] Haifeng Liu, Leigh Tesfatsion, and Ali A Chowdhury. Derivation of locational marginal prices for restructured wholesale power markets. *Journal of Energy Markets*, 2(1):3, 2009.

[38] Saoussen Brini, Hsan Hadj Abdallah, and Abderrazak Ouali. Economic dispatch for power system included wind and solar thermal energy. *Leonardo Journal of Sciences*, 14(2009):204–220, 2009.

[39] N. Augustine, S. Suresh, P. Moghe, and K. Sheikh. Economic dispatch for a microgrid considering renewable energy cost functions. In *2012 IEEE PES Innovative Smart Grid Technologies (ISGT)*, pages 1–7, Jan 2012.

[40] sample residential customer load profile.